Inorganic Chemistry
Article

Inorg. Chem. **2010**, *49*, 10727–10735 **10727**
DOI: 10.1021/ic102004c

Supramolecular Effects on Anion-Dependent Spin-State Switching Properties in Heteroleptic Iron(II) Complexes

Zhaoping Ni and Matthew P. Shores*

Department of Chemistry, Colorado State University, Fort Collins, Colorado 80523-1872, United States

Received September 30, 2010

We describe the preparations, characterizations, and spin-state properties of heteroleptic Fe(II) complexes containing 2,2′-bi-1,4,5,6-tetrahydropyrimidine (H_2bip) and 2-(aminomethyl)pyridine (pic): $[(H_2bip)_2Fe(pic)]X_2$ (X = Br (**1**), BPh_4 (**2**)) and $[(H_2bip)_{1.75}Fe(pic)_{1.25}](BPh_4)_2$ (**3**). The ditopic H_2bip ligand serves as an anion binding group while pic is intended to adjust the Fe(II) ion's ligand field close to the thermal spin-crossover region. The solid state magnetic behavior of each complex salt is found to be heavily influenced by anion and solvate molecules, and is correlated with the first coordination sphere molecular structure, intermolecular interactions, and solvate-induced packing effects. Anion-dependent spin-state switching is observed in dichloromethane solution for samples of **2** treated with ^{n}Bu$_4$NBr, albeit at significantly lower temperatures than what would be expected based on ligand field considerations alone. The origins of this behavior are discussed: circumstantial evidence points to unintended effects of anion-mediated complex pairing in solution as a significant contributor to the lower-than-expected operating temperatures.

Introduction

The spin-crossover (SC) phenomenon represents a prototypical example of molecular switching.[1] When octahedral d^4-d^7 transition-metal complexes feature a properly balanced ligand field, the high-spin (HS) to low-spin (LS) transition (HS→LS) can be driven by external perturbations such as temperature, pressure, or light.[2] Accompanying the spin state change are often drastic transformations in complex color, magnetism, and polarizability. This fundamentally molecular event is being exploited in the production of multifunctional materials, where SC-induced physical changes are combined with other properties synergistically,[3] paving the way for new data storage and display devices.[4]

Increasingly, investigations have sought to tie SC properties to host−guest interactions, since the phenomenon is sensitive to small environmental changes.[5] Understanding and optimizing this link is a necessary step toward using SC-based compounds as chemosensors. Kepert and Murray demonstrated a solvate-induced spin-state change in porous metal−organic frameworks $\{Fe^{II}(L)_2(NCS)_2\}$ (L = bis-pyridyl ligands).[6] Among the more recent examples, the framework compounds $\{Fe^{II}(pz)[M^{II}(CN)_4]\}$ (pz = pyrazine; M = Ni, Pd, Pt) show reversible, spin-state dependent color changes depending on the presence or absence of neutral guest and/or solvate molecules in the solid state.[7]

Recognizing that most Fe(II) SC complexes are cationic,[8] we have focused our efforts on probing cation−anion

*To whom correspondence should be addressed. E-mail: shores@lamar.colostate.edu.

(1) (a) Gütlich, P.; Hauser, A.; Spiering, H. *Angew. Chem., Int. Ed. Engl.* **1994**, *33*, 2024–2054. (b) Sato, O. *Acc. Chem. Res.* **2003**, *36*, 692–700. (c) Bousseksou, A.; Molnár, G.; Matouzenko, G. *Eur. J. Inorg. Chem.* **2004**, 4353–4369.

(2) (a) Hauser, A. *Top. Curr. Chem.* **2004**, *233*, 49–58. (b) Real, J. A.; Gaspar, A. B.; Muñoz, M. C. *J. Chem. Soc., Dalton Trans.* **2005**, 2062–2079.

(3) Gaspar, A. B.; Ksenofontov, V.; Seredyuk, M.; Gütlich, P. *Coord. Chem. Rev.* **2005**, *249*, 2661–2676.

(4) (a) Kahn, O.; Martinez, C. J. *Science* **1998**, *279*, 44–48. (b) *Spin Crossover in Transition Metal Compounds I-III*; Gütlich, P., Goodwin, H. A., Eds.; Springer: Berlin, 2004.

(5) (a) Glaser, T. *Angew. Chem., Int. Ed.* **2003**, *42*, 5668–5670. (b) Nihei, M.; Han, L.; Oshio, H. *J. Am. Chem. Soc.* **2007**, *129*, 5312–5313. (c) Quesada, M.; de la Peña-O'Shea, V. A.; Aromí, G.; Geremia, S.; Massera, C.; Roubeau, O.; Gamez, P.; Reedijk, J. *Adv. Mater.* **2007**, *19*, 1397–1402. (d) Duriska, M. B.; Neville, S. M.; Moubaraki, B.; Cashion, J. D.; Halder, G. J.; Chapman, K. W.; Balde, C.; Létard, J.-F.; Murray, K. S.; Kepert, C. J.; Batten, S. R. *Angew. Chem., Int. Ed.* **2009**, *48*, 2549–2552. (e) Ono, K.; Yoshizawa, M.; Akita, M.; Kato, T.; Tsunobuchi, Y.; Ohkoshi, S.-i.; Fujita, M. *J. Am. Chem. Soc.* **2009**, *131*, 2782–2783.

(6) (a) Halder, G. J.; Kepert, C. J.; Moubaraki, B.; Murray, K. S.; Cashion, J. D. *Science* **2002**, *298*, 1762–1765. (b) Neville, S. M.; Moubaraki, B.; Murray, K. S.; Kepert, C. J. *Angew. Chem., Int. Ed.* **2007**, *46*, 2059–2062. (c) Halder, G. J.; Chapman, K. W.; Neville, S. M.; Moubaraki, B.; Murray, K. S.; Létard, J.-F.; Kepert, C. J. *J. Am. Chem. Soc.* **2008**, *130*, 17552–17562. (d) Neville, S. M.; Halder, G. J.; Chapman, K. W.; Duriska, M. B.; Southon, P. D.; Cashion, J. D.; Létard, J.-F.; Moubaraki, B.; Murray, K. S.; Kepert, C. J. *J. Am. Chem. Soc.* **2008**, *130*, 2869–2876. (e) Neville, S. M.; Halder, G. J.; Chapman, K. W.; Duriska, M. B.; Moubaraki, B.; Murray, K. S.; Kepert, C. J. *J. Am. Chem. Soc.* **2009**, *131*, 12106–12108.

(7) (a) Agustí, G.; Ohtani, R.; Yoneda, K.; Gaspar, A. B.; Ohba, M.; Sánchez-Royo, J. F.; Muñoz, M. C.; Kitagawa, S.; Real, J. A. *Angew. Chem., Int. Ed.* **2009**, *48*, 8944–8947. (b) Ohba, M.; Yoneda, K.; Agustí, G.; Muñoz, M. C.; Gaspar, A. B.; Real, J. A.; Yamasaki, M.; Ando, H.; Nakao, Y.; Sakaki, S.; Kitagawa, S. *Angew. Chem., Int. Ed.* **2009**, *48*, 4767–4771. (c) Southon, P. D.; Liu, L.; Fellows, E. A.; Price, D. J.; Halder, G. J.; Chapman, K. W.; Moubaraki, B.; Murray, K. S.; Létard, J.-F.; Kepert, C. J. *J. Am. Chem. Soc.* **2009**, *131*, 10998–11009.

(8) Halcrow, M. A. *Polyhedron* **2007**, *26*, 3523–3576.

Published on Web 10/22/2010

interactions in solution. Cationic, Fe(II) complexes containing the 2,2′-bi-1,4,5,6-tetrahydropyrimidine (H_2bip) ligand have been shown to change spin state in dichloromethane solution depending on the presence of anions capable of hydrogen-bonding interactions with the bound ditopic ligand. Whereas the homoleptic complex $[Fe(H_2bip)_3]^{2+}$ shows a nearly complete anion-induced HS→LS switching at −40 °C,[9] substitution of one H_2bip ligand with an aromatic diimine (e.g., phenanthroline) moves the switching event in the resulting heteroleptic complex to ambient temperature, albeit with a much higher fraction of LS species in solution.[10] It appears that ligand field balancing via the mixed ligand strategy offers a conceptually straightforward way to obtain spin-state switching chemosensors, one that takes advantage of the vast Fe(II) SC literature precedent.[4b,8]

We seek to understand how this works in greater detail, and to tune anion-dependent spin-state switching in a rational way. Among the questions to be addressed we include: what is the role, if any, of supramolecular interactions in determining complex spin state in solution? Answering this question directly impacts our efforts to employ spin-switching species in chemical sensing applications; it also contributes to understanding cooperativity in SC systems. Cooperativity is one of the most appealing yet elusive concepts in SC phenomena, and is responsible for dramatic changes in magnetic properties in the solid state.[11] The cooperative mechanism strongly depends on intermolecular interactions (e.g., hydrogen bonding, π-stacking). In the solid state, long-range elastic contributions create an "internal pressure" which increases with the concentration of the LS species and interacts equally with all the molecules in the crystal irrespective of distance.[12] In solution, long-range interactions are disrupted by solvent molecules, but in principle it is easier to spectroscopically probe individual (e.g., cation−anion) interactions. In addition, possible aggregation or other clustering of SC-capable complexes can be monitored, thus providing a microscopic, complementary picture of factors contributing to cooperativity.

In this regard, the 2-(aminomethyl)pyridine (pic) ligand avails itself as a suitable companion for H_2bip, since it features a stronger ligand field;[13] in addition, homoleptic $[Fe(pic)_3]^{2+}$ complexes are known to have SC properties.[14] We would expect to find that heteroleptic complexes containing both ligands would show anion-induced state changes at higher temperatures than that encountered for $[Fe(H_2bip)_3]^{2+}$, but perhaps a complete HS→LS transition as opposed to the weaker spin response encountered for $[(H_2bip)_2Fe(phen)]^{2+}$. This latter point is important in that it is preferable to probe the full range of SC behavior instead of being limited to "mostly" LS or HS species.

Herein, we report the preparations and representative anion titration studies on heteroleptic $[(H_2bip)_{2-n}Fe(pic)_{1+n}]^{2+}$ complexes. Whereas the solid state magnetic behavior is heavily influenced by both anion and solvent species, the solution behavior shows anion-dependent spin-state switching properties, albeit at temperatures significantly *lower* than what is predicted by simple ligand field calculations. The origins of this behavior are explored, and linked to supramolecular interactions mediated by the ancillary pic ligand both in the solid state and in solution.

Experimental Section

Preparation of Compounds. All manipulations of iron complexes were performed inside a dinitrogen-filled glovebox (MBRAUN Labmaster 130). All non-deuterated solvents were sparged with dinitrogen, passed over alumina, and subjected to three freeze−pump−thaw cycles to remove dissolved oxygen. The ligand 2,2′-bi-1,4,5,6-tetrahydropyrimidine (H_2bip) was prepared according to literature precedent.[13b] The precursor complex $[(H_2bip)_2FeBr_2]$ was synthesized according to our previous report.[10] All other compounds and reagents were obtained commercially and used as received.

$[(H_2bip)_2Fe(pic)]Br_2\cdot 0.25CH_2Cl_2$ (1a). To a solution of $[(H_2bip)_2FeBr_2]$ (391 mg, 0.713 mmol) in 15 mL of methanol was added a solution of pic (78 mg, 0.714 mmol) in 6 mL of methanol. The solution was stirred for an additional 30 min at room temperature before the solvent was removed in vacuo. The solid was extracted into dichloromethane (7 mL), as the complex $[(H_2bip)_2FeBr_2]$ has low solubility in CH_2Cl_2. The mixture was filtered, and the filtrate was evaporated to obtain the complex salt as a free-flowing powder. This solid was washed with 15 mL of diethyl ether and dried under vacuum at room temperature for 6 h, affording 461 mg of powdered product (95%). IR (KBr): ν_{N-H} 3234, 3123 cm^{-1}. Absorption spectrum (CH_2Cl_2): λ_{max} (ε_M) 459 nm (1520 $L\cdot mol^{-1}\cdot cm^{-1}$). ^1H NMR (CD_2Cl_2) δ 81.2, 78.4, 66.2, 43.2, 40.5, 38.9, 32.7, 23.2, 18.5, 15.2, 12.5, 8.7, 2.3, −9.8 ppm. Anal. Calcd for $C_{22.25}H_{36.5}N_{10}Br_2Cl_{0.5}Fe$: C, 39.45; H, 5.43; N, 20.67. Found: C, 39.52; H, 5.55; N, 20.55.

$[(H_2bip)_2Fe(pic)]Br_2\cdot 0.5CH_3OH$ (1b). Crystals of this compound were grown by slow diffusion (∼4 days) of diethyl ether into a dilute methanolic solution (∼10 mM) of **1a**. The crystals were dried under vacuum at room temperature for 15 min to remove trace amounts of diethyl ether. Yield: 64%. IR (KBr): ν_{N-H} 3249, 3135 cm^{-1}. Anal. Calcd for $C_{22.5}H_{38}N_{10}O_{0.5}Br_2Fe$: C, 40.20; H, 5.70; N, 20.84. Found: C, 40.45; H, 5.46; N, 21.06.

$[(H_2bip)_2Fe(pic)]Br_2$ (1c). Microcrystals of this compound were grown by relatively quick diffusion (∼1.5 days) of diethyl ether into a concentrated methanolic solution (∼40 mM). The crystals were dried under vacuum at room temperature for 15 min to remove trace amounts of diethyl ether. Yield: 76%. IR (KBr): ν_{N-H} 3225, 3119 cm^{-1}. Anal. Calcd for $C_{22}H_{36}N_{10}Br_2Fe$: C, 40.27; H, 5.53; N, 21.34. Found: C, 40.21; H, 5.53; N, 21.62.

$[(H_2bip)_2Fe(pic)](BPh_4)_2$ (2). A solution of **1a** (210 mg, 0.310 mmol) in 8 mL of methanol was added dropwise to a solution of $NaBPh_4$ (438 mg, 1.267 mmol) in 10 mL of methanol, resulting in the formation of a khaki-colored precipitate. The mixture was stirred for an additional 30 min at room temperature. The solid was collected by filtration, washed with methanol (10 mL) and diethyl ether (10 mL), and dried under vacuum at room temperature for 6 h to obtain 305 mg **2** as a powdered product (87%). IR (KBr): ν_{N-H} 3390, 3329, 3278 cm^{-1}. Absorption spectrum (CH_2Cl_2): λ_{max} (ε_M) 412 nm (1090 $L\cdot mol^{-1}\cdot cm^{-1}$). ^1H NMR (CD_2Cl_2) δ 90.3, 85.3, 79.8, 72.8, 53.5, 46.6, 45.8, 42.8, 39.7, 30.5,

(9) Ni, Z.; Shores, M. P. *J. Am. Chem. Soc.* **2009**, *131*, 32–33.
(10) Ni, Z.; McDaniel, A. M.; Shores, M. P. *Chem. Sci.* **2010**, *1*, 615–621.
(11) Real, J. A.; Gaspar, A. B.; Niel, V.; Muñoz, M. C. *Coord. Chem. Rev.* **2003**, *236*, 121–141.
(12) (a) Spiering, H.; Kohlhaas, T.; Romstedt, H.; Hauser, A.; Bruns-Yilmaz, C.; Kusz, J.; Gütlich, P. *Coord. Chem. Rev.* **1999**, *190−192*, 629–647. (b) Hauser, A.; Jeftic, J.; Romstedt, H.; Hinek, R.; Spiering, H. *Coord. Chem. Rev.* **1999**, *190−192*, 471–491.
(13) (a) Sutton, G. J. *Aust. J. Chem.* **1960**, *13*, 74–79. (b) Burnett, M. G.; McKee, V.; Nelson, S. M. *J. Chem. Soc., Dalton Trans.* **1981**, 1492–1497.
(14) (a) Hostettler, M.; Törnroos, K. W.; Chernyshov, D.; Vangdal, B.; Bürgi, H.-B. *Angew. Chem., Int. Ed.* **2004**, *43*(35), 4589–4594. (b) Chernyshov, D.; Vangdal, B.; Törnroos, K. W.; Bürgi, H. B. *New J. Chem.* **2009**, *33*, 1277–1282. (c) Törnroos, K. W.; Hostettler, M.; Chernyshov, D.; Vangdal, B.; Bürgi, H. B. *Chem.—Eur. J.* **2006**, *12*, 6207–6215. (d) Chernyshov, D.; Hostettler, M.; Tornroos, K. W.; Bürgi, H. B. *Angew. Chem., Int. Ed.* **2003**, *42*, 3825–3830. (e) Greenaway, A. M.; Sinn, E. *J. Am. Chem. Soc.* **1978**, *100*, 8080–8084. (f) Renovitch, G. A.; Baker, W. A. *J. Am. Chem. Soc.* **1967**, *89*, 6377–6378.

Table 1. Crystallographic Data[a] for Compounds $[(H_2bip)_2Fe(pic)]Br_2 \cdot 0.5CH_3OH$ (**1b**), $[(H_2bip)_2Fe(pic)]Br_2$ (**1c**), and $[(H_2bip)_{1.75}Fe(pic)_{1.25}](BPh_4)_2 \cdot 0.1CH_2Cl_2$ (**3**)

	1b·LT	**1b·RT**	**1c·RT**	**3·LT**	**3·RT**
formula	$C_{22.5}H_{38}N_{10}O_{0.5}Br_2Fe$	$C_{22.5}H_{38}N_{10}O_{0.5}Br_2Fe$	$C_{22}H_{36}N_{10}Br_2Fe$	$C_{69.5}H_{74.5}N_{9.5}B_2Fe$	$C_{69.5}H_{74.5}N_{9.5}B_2Fe$
fw	672.26	672.26	656.26	1120.36	1120.36
color	orange-red	orange red	orange red	yellow	yellow
habit	block	block	needle	block	block
T, K	100	296	296	100	296
space group	$P2_1/c$	$P2_1/c$	$P2_1/n$	$P2_1/c$	$P2_1/c$
Z	4	4	4	4	4
a, Å	15.7706(7)	16.1436(14)	9.6909(1)	21.3900(3)	21.5986(4)
b, Å	9.8001(4)	10.0387(9)	12.8600(2)	14.5330(2)	14.6795(3)
c, Å	18.4582(8)	18.7854(16)	25.1560(3)	20.3121(3)	20.5912(3)
α, deg	90	90	90	90	90
β, deg	105.885(2)	104.886(2)	96.454(1)	105.614(1)	105.665(1)
γ, deg	90	90	90	90	90
V, Å^3	2743.8(2)	2942.2(4)	3115.20(7)	6081.22	6286.1(2)
d_{calc}, g/cm^3	1.623	1.513	1.399	1.224	1.184
GOF	1.048	0.957	1.022	1.060	1.065
$R_1(wR_2)^b$	3.90(10.40)	4.81(11.00)	4.65(12.23)	6.56(19.10)	6.79(22.42)

[a] Obtained with graphite-monochromated Mo Kα ($\lambda = 0.71073$ Å) radiation. [b] $R_1 = \sum||F_o| - |F_c||/\sum|F_o|$, $wR_2 = \{\sum w(F_o^2 - F_c^2)^2/\sum w(F_o^2)^2\}^{1/2}$ for $F_o > 4\sigma(F_o)$.

23.9, 22.7, 18.6, 13.1, 10.2 (BPh_4), 9.2 (BPh_4), 8.8 (BPh_4), 6.9, 1.8 ppm. Anal. Calcd for $C_{70}H_{76}N_{10}B_2Fe$: C, 74.08; H, 6.75; N, 12.34. Found: C, 74.01; H, 6.46; N, 12.23.

$[(H_2bip)_{1.75}Fe(pic)_{1.25}](BPh_4)_2 \cdot 0.1CH_2Cl_2$ (3). Crystals suitable for X-ray analysis were grown by diffusion of diethyl ether into a dilute solution (~1 mM) of **2** in 6:1 dichloromethane/diethyl ether mixture over one week. The crystals were dried under vacuum at room temperature for 15 min to remove trace amounts of diethyl ether. IR (KBr): ν_{N-H} 3401, 3342, 3291 cm^{-1}. Anal. Calcd for $C_{69.6}H_{74.7}N_{9.5}B_2Cl_{0.2}Fe$: C, 74.05; H, 6.67; N, 11.79. Found: C, 73.89; H, 6.59; N, 12.09.

X-ray Structure Determinations. Structures were determined for the compounds listed in Table 1. All single crystals were coated in Paratone-N oil prior to removal from the glovebox. The crystals were supported on Cryoloops before being mounted on a Bruker Kappa Apex II CCD diffractometer under a stream of dinitrogen. Data were collected with Mo K_α radiation and a graphite monochromator. Initial lattice parameters were determined from a minimum of 266 reflections harvested from 36 frames, and data sets were collected targeting complete coverage and 4-fold redundancy. Data were integrated and corrected for absorption effects with the Apex II software package.[15] Structures were solved by direct methods and refined with the SHELXTL software package.[16] Thermal parameters for all non-hydrogen atoms were refined anisotropically with the exception of disordered atoms as noted in the respective cif files. Hydrogen atoms were added at the ideal positions and were refined using a riding model where the thermal parameters were set at 1.2 times those of the attached carbon atom. Specific details concerning structure refinement can be found in the supplementary crystallographic files. Positional disorder was found for some of the aliphatic carbon atoms of the H_2bip ligands in **1b**, **1c**, and **3**; these were modeled with partial occupancies over two sites using isotropic thermal parameters. Compositional disorder was found for one chelating ligand in **3**, with the ratio of H_2bip/pic refining to 75:25. After numerous refinement attempts failed, severe solvent disorder in the structures of **1c** (~0.15 diethyl ether) and **3** (~0.38 CH_2Cl_2) necessitated the use of SQUEEZE[17] to remove the disordered components and achieve reasonable refinements. In support of the SQUEEZE results, elemental analyses performed on the dried (room temperature, 15 min) crystalline products indicates that all of the diethyl ether in **1c** and a portion of the CH_2Cl_2 in **3** (0.28 equiv) can be removed during this process. All other characterizations are based on these dried crystals. The parameters presented in Table 1 for **1c** and **3** reflect solvent-free data.

Magnetic Susceptibility Measurements. All samples (solid state or solution) were prepared under a dinitrogen atmosphere. Finely ground solid samples were loaded into gelatin capsules and inserted into straws for analysis. The straws were sealed in a Schlenk tube for transportation between the glovebox and magnetometer, and were quickly loaded into the instrument to minimize exposure to air. Solid state magnetic susceptibility measurements were performed with a Quantum Design model MPMS-XL superconducting quantum interference device (SQUID) magnetometer in the temperature range of 5 to 300 K under a measuring field of 1000 G. The data were corrected for the magnetization of the sample holder by subtracting the measured susceptibility of an empty sample holder. Diamagnetic corrections were applied by using Pascal's constants.[18] Magnetic susceptibilities in CD_2Cl_2 solution were determined by the Evans method using TMS as the reference.[19] ^{1}H NMR spectra were recorded using Varian INOVA instruments operating at 300 or 400 MHz. Solvent density corrections with temperature were carried out according to the correction data provided for CH_2Cl_2.[20] Data were corrected for diamagnetic contributions of the iron complex using Pascal's constants;[18] diamagnetic contributions of the solvent were ignored, in accord with literature precedent.[21]

Anion Binding Studies. The titration of **2** with bromide (as ^{n}Bu$_4$NBr) was carried out according to our previous report.[10]

(a) Titrations Monitored by ^{1}H NMR Spectroscopy. Titrations were performed on **2** in CD_2Cl_2 using host concentrations of 7.5 mM. Stock solutions of ^{n}Bu$_4$NBr were prepared in dichloromethane at concentrations 10 times that of the host solution. To avoid dilution effects, an air-free NMR tube was charged with the guest solution in aliquots via a 100 μL syringe (25−250 μL, up to 5 equiv of Br^- anion were added for 0.5 mL host solution), and the solvent was carefully removed in vacuo. Then the host solution was added, and ^{1}H NMR spectra were obtained. Diamagnetic corrections for the host complex and added ^{n}Bu$_4$NBr were applied.[10]

(b) Titrations Monitored by Electronic Absorption Spectroscopy. Stock solutions of the host **2** were prepared in dichloromethane (0.36 mM). Stock solutions of the guest bromide

(15) *APEX 2*; Bruker Analytical X-Ray Systems, Inc.: Madison, WI, 2008.
(16) Sheldrick, G. M. *SHELXTL*, Version 6.14; Bruker Analytical X-Ray Systems, Inc.: Madison, WI, 1999.
(17) Sluis, P. v. d.; Spek, A. L. *Acta Crystallogr.* **1990**, *A46*, 194–201.
(18) Kahn, O. *Molecular Magnetism*; VCH: New York, 1993.
(19) (a) Evans, D. F. *J. Chem. Soc.* **1959**, 2003–2005. (b) Ostfeld, D.; Cohen, I. A. *J. Chem. Educ.* **1972**, *49*, 829. (c) Grant, D. H. *J. Chem. Educ.* **1995**, *72*, 39.
(20) Yaws, C. L. *Thermodynamic and Physical Property Data*; Gulf Publishing Co.: Houston, 1992; p 96.
(21) Grant, D. H. *J. Chem. Educ.* **1995**, *72*, 39.

species were prepared by dissolving approximately 100 equiv of $^{n}Bu_4NBr$ into the stock solution of the host. Titration data were collected after sequential additions of the guest solution (5−40 μL via a 100 μL syringe, up to 11 equiv of Br^- in total) to a 4 mL host solution in an air-free glass spectrometric cell.

Other Physical Measurements. UV−visible spectra were recorded on an Agilent 8453 spectrophotometer in an air-free glass cell. Infrared spectra were measured under a dinitrogen flow with a Nicolet 380 FT-IR using KBr pellets. Representative samples collected in fluorolube oil mull as well as by ATR give the same resonances, with some slight differences in intensity (Supporting Information, Figure S1). Elemental analyses were performed by Robertson Microlit Laboratories Inc. in Madison, NJ.

Results and Discussion

Syntheses and Solid State Characterizations. The pic species was chosen to pair with H_2bip because of its favorable ligand field characteristics. In practice, a direct measure of the ligand field strength in Fe(II) diimine complexes is usually not available because of the presence of charge-transfer bands that overlap the weaker ligand field bands. Fortunately, as reported by Busch, the HS Fe(II) ligand field parameters can be roughly correlated with Ni(II) analogues.[22] According to Goodwin, if SC in a homoleptic Fe(II) species is to be observed, the ligand field value (D_q = $0.1\Delta_o$) of Ni(II) analogues generally falls in the range 1120−1240 cm^{-1}.[23] The Ni(II) D_q values for H_2bip and pic are 1100 and 1163 cm^{-1}, respectively.[13] Guided by the above-mentioned experiential rules, we hypothesize that the complex with a 2:1 H_2bip/pic ratio should exhibit a D_q value of approximately 1121 cm^{-1}, placing it in the SC-capable regime.

Analytically pure, powdered samples of $[(H_2bip)_2Fe(pic)]Br_2\cdot 0.25CH_2Cl_2$ (**1a**) and $[(H_2bip)_2Fe(pic)](BPh_4)_2$ (**2**) are produced in excellent yields from the precursor complex $[(H_2bip)_2FeBr_2]$ by simple ligand substitution (followed by ion exchange to obtain **2**). The bromide salt of $[(H_2bip)_2Fe(pic)]^{2+}$ can be crystallized with partial methanol (**1b**) and trace ether (**1c**) solvate molecules. In contrast, a structure of the pure tetraphenylborate salt **2** has not been obtained; instead, $[Fe(H_2bip)_{1.75}(pic)_{1.25}](BPh_4)_2$ (**3**) is crystallized over a period of one week from dilute dichloromethane solutions of **2**, indicating that ligand scrambling is operative, albeit slowly, even in relatively nonpolar solvents. On the basis of X-ray structural data (vide infra), **3** can be formulated as the mixed cation salt $[(H_2bip)_2Fe(pic)]_{0.75}\cdot[(H_2bip)Fe(pic)_2]_{0.25}(BPh_4)_2$; this compound contains a small amount of highly disordered dichloromethane solvate.

The solid state magnetic susceptibilities for **1**−**3** appear to reflect both ligand field and solvate considerations (Figure 1). Considering the bromide salts as a group, they cut a wide swath in SC space. The powder sample **1a** shows a slow and incomplete spin crossover: $\chi_M T$ registers at 3.11 emu·K·mol^{-1} at 300 K, as expected for mostly-HS Fe(II), decreases gradually to 1.00 emu·K·mol^{-1} at 75 K, remains fairly constant with decreasing temperature until 30 K, then further cooling to 5 K leads to a $\chi_M T$ value equal to 0.64 emu·K·mol^{-1}. Magnetic susceptibility measurements for the methanol solvate-containing crystal sample

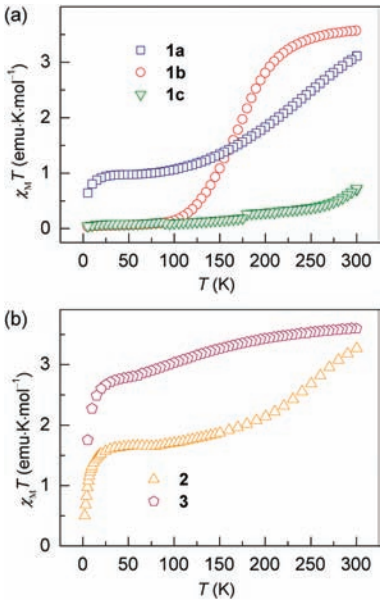

Figure 1. Temperature dependence of the solid-state magnetic susceptibilities for (a) the bromide salts **1a**−**1c**, and (b) tetraphenylborate salts **2** and **3**, obtained under a measuring field of 1000 G.

1b show a gradual albeit complete spin-state change: $\chi_M T$ varies from 3.57 emu·K·mol^{-1} at 300 K to 0.03 emu·K·mol^{-1} at 5 K, with a spin-transition temperature ($T_{1/2}$) of 173 K. In contrast, the $\chi_M T$ value of the "solvent free" crystal **1c**, 0.72 emu·K·mol^{-1} at 300 K, indicates a predominantly LS state even at room temperature.

Meanwhile, the tetraphenylborate salts **2** and **3** shift toward the HS portion of SC space. The powder sample **2** transitions from HS to LS very gradually and incompletely: $\chi_M T$ decreases from 3.27 emu·K·mol^{-1} at 300 K to 1.65 emu·K·mol^{-1} at 80 K, and then remains fairly constant with decreasing temperature until 25 K. The sudden decrease below 25 K is indicative of a magnetically anisotropic HS Fe(II) ion.[5b] On the basis of $\chi_M T$ values alone, it is tempting to interpret this behavior as consistent with multiple spin centers in **2**, some which are SC-capable and others that are HS at all temperatures; however we currently lack structural data that would confirm this conjecture. Somewhat confounding to us, the mixed-cation complex salt **3**, which contains a higher proportion of the stronger field pic ligand, actually remains HS throughout the temperature range probed, dropping off only at very low temperatures because of magnetic anisotropy considerations.

On the basis of solid state magnetometry data alone, we cannot immediately confirm that stronger field ligand incorporation can increase spin-transition temperatures. On one hand, comparing **2** with $[Fe(H_2bip)_3](BPh_4)_2$, pic ligand substitution successfully moves the mixed ligand field into the SC regime. On the other hand, the bromide salt **1a** may or may not enjoy a stronger ligand field than the homoleptic $[Fe(H_2bip)_3]Br_2$ complex salt—the presence of solvate molecules muddles straightforward interpretation.

Since SC properties in general depend on intermolecular interactions,[24] vibrational spectra may aid the interpretation

(22) Robinson, M. A.; Curry, J. D.; Busch, D. H. *Inorg. Chem.* **1963**, *2*, 1178–1181.
(23) Goodwin, H. A. *Top. Curr. Chem.* **2004**, *233*, 59–90.
(24) Gütlich, P.; Garcia, Y.; Goodwin, H. A. *Chem. Soc. Rev.* **2000**, *29*, 419–427.

Table 2. Selected Bond Distances (Å), Angles (deg) and Distortion Parameters (deg)[a]

	1b·RT	**1b·LT**	**1c·RT**	**3·RT**	**3·LT**
Fe−N(H_2bip)	2.147(5)	1.990(2)	1.997(3)	2.174(3)[b]	2.124(3)[b]
Fe−N(pyridine)	2.222(5)	1.978(2)	1.990(3)	2.218(3)[b]	2.157(3)[b]
Fe−N(amine)	2.207(4)	2.034(2)	2.039(3)	2.230(3)[b]	2.171(3)[b]
Fe−N(pic)	2.215(5)	2.006(2)	2.015(3)	2.224(3)[b]	2.164(3)[b]
Fe−N(avg)	2.169(5)	1.995(2)	2.003(3)	2.188(5)	2.133(5)
Σ	93.27(18)	60.98(7)	65.58(12)	104.43(13)	97.01(12)
Θ	248.5	155.8	137.1	263.1	244.8

[a] For determinations of Σ and Θ, see references 25 and 26. [b] Excluding the compositionally disordered ligand site.

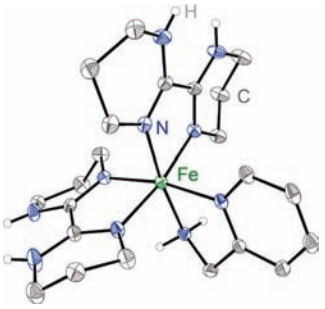

Figure 2. Crystal structure of the cation in **1b** at 100 K, rendered with 40% probability ellipsoids. Green, blue, and gray ellipsoids represent Fe, N, and C atoms, respectively; gray spheres denote H atoms bound to N atoms; other H atoms and disordered minor components are omitted for clarity.

of the magnetic data. Here, resonances tentatively assigned to N−H stretching modes can probe ambient temperature hydrogen bonding between complex cations and anions. The "solvent free" crystal **1c** shows the lowest energy ν_{N-H} resonances (3234 and 3123 cm^{-1} for **1a**, 3249 and 3135 cm^{-1} for **1b** and 3225 and 3119 cm^{-1} for **1c**, respectively), which indicates strong hydrogen bonding to bromide, resulting in the largely LS state at room temperature. Powder **1a** and crystal **1b** show weaker hydrogen bonding interactions, consistent with their higher spin states at room temperature, albeit much stronger than compounds **2** and **3**. In all, the ambient temperature ν_{N-H} modes appear to be qualitatively correlated not only to observed spin state but to the sharpness of the eventual solid-state spin-transition profile.

Single-crystal X-ray analyses were performed to explore magneto-structural relationships in greater detail. Relevant bond distances, angles, and distortion parameters are presented in Table 2. Analysis of the bromide salt with methanol solvate **1b** obtained at 296 and 100 K (**1b·RT** and **LT**) reveal structures of Fe(II) complexes in HS and LS states, respectively. Each Fe(II) ion is found in a distorted octahedral coordination environment, coordinated by two H_2bip ligands and one pic ligand (Figure 2). The crystallographic data of **1b·RT** and **1b·LT** are similar to each other, and no crystallographic phase transition occurs. The unit cell volume is reduced by ∼7% as the temperature is reduced from 296 to 100 K. The average Fe−N distance at ambient temperature is consistent with HS Fe(II) ions, and the average Fe−N distance of **1b·LT** is more typical for LS Fe(II). The structural characterization of the "solvent-free" crystal **1c·RT** (at 296 K) is in line with what is usually observed for LS Fe(II) complexes, with an average Fe−N

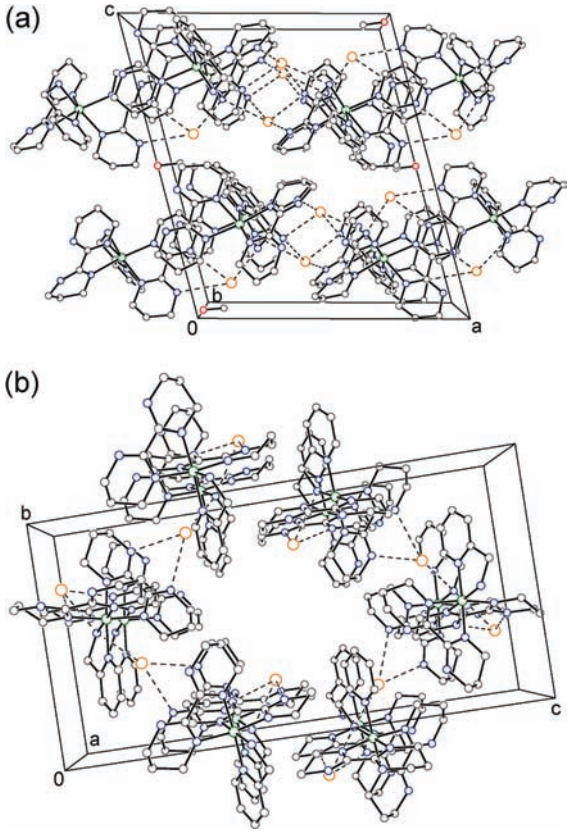

Figure 3. Crystal packing diagrams of (a) **1b·LT**, viewed down the *b* axis; and (b) **1c**, viewed along the *a* axis. H atoms and disordered components are omitted for clarity. Dotted lines indicate hydrogen bonding interactions. H-bonding between MeOH and Br^- in (a) have been omitted for clarity.

distance of 2.003(3) Å. Structural distortions of the Fe(II) first coordination sphere (Σ and Θ parameters[25,26]) are also consistent with the spin-state assignments derived from bond length analysis (Table 2).

Comparing the structures of the two isolated bromide salts **1b** and **1c**, the immediate hydrogen bonding environments are very similar (see Supporting Information, Table S1). Each H_2bip ligand chelates a bromide, and each amine moiety of pic interacts with two bromides. In turn, all bromide anions are most closely associated with two complex cations. In the structures of **1b**, there are additional interactions between half of the bromides (Br1) and the partially occupied and disordered solvate methanol molecules.

Although local interactions are similar, the spin states of the Fe(II) ions in the ambient temperature structures of **1b** and **1c** are different. This is somewhat counterintuitive given that **1b·RT** has a smaller unit cell volume than **1c** for the same number of Fe(II) complexes, and the shorter Fe−L bond distances in LS complexes might be expected to result in smaller unit cells. The reason may be linked to the *extended* H-bonding network, which the crystal

(25) (a) Drew, M. G. B.; Harding, C. J.; McKee, V.; Morgan, G. G.; Nelson, J. *J. Chem. Soc., Chem. Commun.* **1995**, 1035–1038. (b) Guionneau, P.; Marchivie, M.; Bravic, G.; Létard, J.-F.; Chasseau, D. *J. Mater. Chem.* **2002**, *12*, 2546–2551.

(26) Marchivie, M.; Guionneau, P.; Létard, J.-F.; Chasseau, D. *Acta Crystallogr.* **2005**, *B61*, 25–28.

packing diagrams for **1b·RT** and **1c** illustrate nicely (Figure 3). For **1b·RT**, electrically neutral $[(H_2bip)_2$-Fe(pic)$]Br_2$ layers parallel to the *ab* plane are spaced apart along the *c* axis by methanol solvate molecules to form a three-dimensional H-bonding network. For **1c**, columns of complex cations along the *a* axis interact with bromide anions to form undulating layers, leaving columns of ether solvate/void space along *a* (Figures 3b and S5). Comparing **1b·RT** and **1c**, the range of Fe···Fe distances is larger in **1b·RT** than in **1c** (9.269(1)—10.290(2) and 8.445(1)—9.691(1) Å, respectively, see Supporting Information, Table S2), **1b·RT** has fewer "shorter" contacts, and the average Fe···Fe distances are actually longer in **1b·RT** than in the less dense **1c** (9.791(1) versus 9.031(1) Å, respectively). We speculate that since bromide in **1b·RT** can satisfy H-bonding requirements by interacting with the complex cations and methanol solvate, a more flexible three-dimensional (3D) H-bonding network is formed: the flexibility allows for SC properties to emerge as a function of temperature, while the 3D nature of the interactions gives rise to a sharper spin transition. In contrast, bromide anions in **1c** are restricted to the H_2bip and pic ligands for bonding partners, resulting in a quasi two-dimensional network that is actually more sterically constraining to the Fe(II) ions than the environment in **1b·RT**; thus, the Fe(II) ions in **1c** are locked into the LS state even at room temperature.[27]

Supramolecular effects on observed spin state are also evident in the mixed cation heteroleptic complex $[Fe(H_2bip)_{1.75}(pic)_{1.25}](BPh_4)_2$ (**3**). The complex features one each of fully occupied H_2bip and pic ligands, and compositional disorder in the third chelating ligand, with the H_2bip/pic ratio refining to 75:25. The average Fe−N distances in **3** are indicative of HS Fe(II) ions. Compared with **1b·RT**, they all show relatively larger Σ and Θ values, which is consistent with the HS state. Weak hydrogen bonding interactions between the cation and BPh_4^- anions are observed (the shortest NH···BPh_4 contact is 3.274(4) Å at 100 K). Thus, the cations are effectively blocked from each other by the BPh_4^- anions and the shortest intermolecular Fe···Fe distance is 10.965(1) Å at 100 K. Interestingly, the increased presence of the stronger field pic ligand cannot overcome the lack of intermolecular interactions, such that of the five compounds studied here, the magnetism of **3** tends most toward the HS regime.

In sum, we find that solid state magnetic interpretation of these compounds is complicated by solvate molecules and packing considerations; nevertheless, the wide range of spin behaviors observed demonstrates that the ligand field of the heteroleptic complex $[(H_2bip)_2Fe(pic)]^{2+}$ is precariously balanced in the SC-capable regime, even at 296 K. This would suggest to us that the complex is poised to report subtle environmental changes (e.g., anion binding) via spin-state changes at ambient temperatures.

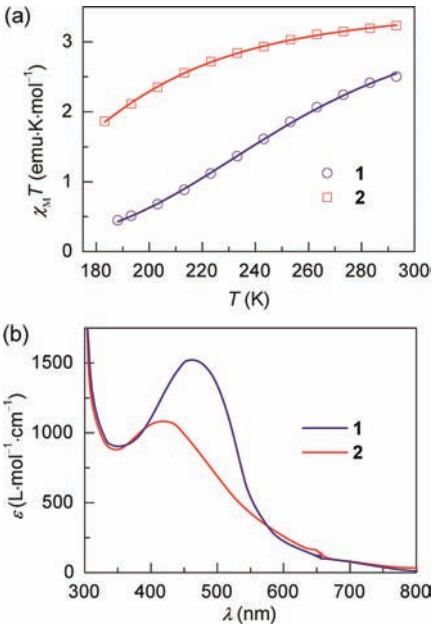

Figure 4. (a) Temperature dependence of the magnetic susceptibilities of complex salts **1** and **2** in CD_2Cl_2 solution and curves fit to eq 1; (b) electronic absorption spectra of **1** and **2** in a CH_2Cl_2 solution at 296 K.

Solution Characterization. Relative to the solid state, we might expect more straightforward behavior for the heteroleptic complex salts in solution, since long-range intermolecular interactions are broken up by solvent molecules. The magnetic susceptibilities for **1c** and **2** were determined in CD_2Cl_2 solution over a 183−296 K range using Evans' method,[19] and plots of $\chi_M T$ versus *T* are collected in Figure 4a. Unlike the solid state experiment, $\chi_M T$ for the bromide salt **1** gradually decreases from 2.51 emu·K·mol^{-1} at 296 K, with LS fraction $\gamma_{LS} = 0.26$,[28] to 0.45 emu·K·mol^{-1} ($\gamma_{LS} = 0.87$) at 188 K. For the tetraphenylborate salt **2**, the spin-transition curve is even more gradual: $\chi_M T$ decreases from 3.24 emu·K·mol^{-1} ($\gamma_{LS} = 0.04$) at 296 K to 1.87 emu·K·mol^{-1} ($\gamma_{LS} = 0.45$) at 183 K. Thus, both salts show SC properties in dichloromethane solution, and the more strongly interacting bromide salt **1** achieves a higher population of LS species at higher temperatures compared to **2**, in accordance with ligand field expectations and previous results.[9,10] The largest $\chi_M T$ difference between the BPh_4^- and Br^- salts ($\Delta_{\chi T} = 1.67$ emu·K·mol^{-1}) occurs at 203 K. Based solely on the fact that pic imparts a stronger ligand field than H_2bip, we would expect this anion-dependent spin-state switching to occur at *higher* temperatures than what is found for $[Fe(H_2bip)_3]^{2+}$.[9] Instead, $[(H_2bip)_2$-Fe(pic)$]^{2+}$ appears to operate at temperatures ~30 °C *lower* than the homoleptic complex.

To verify that the observed spin-state changes are due to spin crossover within the heteroleptic complex, and not solvolysis products from ligand dissociation, thermodynamic

(27) (a) Matouzenko, G. S.; Bousseksou, A.; Lecocq, S.; van Koningsbruggen, P. J.; Perrin, M.; Kahn, O.; Collet, A. *Inorg. Chem.* **1997**, *36*, 5869–5879. (b) Niel, V.; Gaspar, A. B.; Munoz, M. C.; Abarca, B.; Ballesteros, R.; Real, J. A. *Inorg. Chem.* **2003**, *42*, 4782–4788. (c) Galet, A.; Munoz, M. C.; Gaspar, A. B.; Real, J. A. *Inorg. Chem.* **2005**, *44*, 8749–8755. (d) Reger, D. L.; Gardinier, J. R.; Smith, M. D.; Shahin, A. M.; Long, G. J.; Rebbouh, L.; Grandjean, F. *Inorg. Chem.* **2005**, *44*, 1852–1866. (e) Galet, A.; Gaspar, A. B.; Muñoz, M. C.; Levchenko, G.; Real, J. A. *Inorg. Chem.* **2006**, *45*, 9670–9679. (f) Reger, D. L.; Gardinier, J. R.; Elgin, J. D.; Smith, M. D.; Hautot, D.; Long, G. J.; Grandjean, F. *Inorg. Chem.* **2006**, *45*, 8862–8875. (g) Costa, J. S.; Lappalainen, K.; de Ruiter, G.; Quesada, M.; Tang, J.; Mutikainen, I.; Turpeinen, U.; Grunert, C. M.; Gütlich, P.; Lazar, H. Z.; Létard, J.-F.; Gamez, P.; Reedijk, J. *Inorg. Chem.* **2007**, *46*, 4079–4089. (h) Sheu, C.-F.; Pillet, S. b.; Lin, Y.-C.; Chen, S.-M.; Hsu, I. J.; Lecomte, C.; Wang, Y. *Inorg. Chem.* **2008**, *47*, 10866–10874.

(28) LS and HS fractions are determined by assuming that the limiting LS and HS $\chi_M T$ (also Curie constant) values are 0 and 3.38 emu·K·mol^{-1}, respectively.

Table 3. Thermodynamic Parameters for **1** and **2** in CD_2Cl_2[a]

	TIP_{HS} ($emu \cdot mol^{-1}$)	TIP_{LS} ($emu \cdot mol^{-1}$)	ΔH ($kJ \cdot mol^{-1}$)	ΔS ($J \cdot mol^{-1} \cdot K^{-1}$)	T_C (K)
1	0.0006	0.0005(2)	13.6(3)	54	252(2)
2	0.0006(1)	0.0005	9.7(2)	54	180(1)

[a] The g_{HS} value is fixed at 2.11;[29b] TIP values without esds are fixed manually.

parameters were estimated by fits of the variable temperature $\chi_M T$ data to the following:

$$\chi T = \frac{\left[\frac{g_{HS}^2}{4} C_{HS} + TIP_{HS} \times T\right] - \left[\frac{g_{LS}^2}{4} C_{LS} + TIP_{LS} \times T\right]}{1 + \exp\left[\frac{\Delta H}{R} \times \left(\frac{1}{T} - \frac{1}{T_c}\right)\right]} + \left[\frac{g_{LS}^2}{4} C_{LS} + TIP_{LS} \times T\right] \quad (1)$$

where g, C, and TIP are the Landé factor, Curie constant, and temperature-independent paramagnetism terms of the $S = 2$ (HS, and $S = 0$ (LS) states, respectively;[28] R is the gas constant; ΔH is the enthalpy term; and T_c is the spin-transition temperature (where HS/LS = 50:50). The entropy term is calculated from the expression $\Delta S = \Delta H/T_c$.[29] The fitting results are summarized in Table 3. We note that the magnetism of HS Fe(II) complexes can deviate from Curie behavior, so these results should be viewed as estimates. The thermodynamic quantities obtained for **1** are typical for SC Fe(II) complexes.[1a] The smaller enthalpy change for **2** is consistent with a less complete SC behavior, which is affected by the much reduced H-bonding ability of BPh_4^- relative to Br^-. According to literature precedent, the small ΔH values found here apparently exclude any obvious ligand dissociation processes occurring during the experiment.[30]

However, we note that the actual ^1H NMR spectra of the various salts are more complicated than anticipated (Supporting Information, Figures S8 and S9), even accounting for the low symmetry imparted by the pic ligand. Efforts to assign resonances to specific protons are hampered by paramagnetic broadening and shifting, and by the presence of overlapping peaks. The spectra of all the bromide salts **1a**−**c** are identical, indicating that the small amounts of co-crystallized solvent do not affect solution properties. Meanwhile, analytically pure compound **2** has virtually identical chemical shifts as found for the mixed-cation compound **3** (Supporting Information, Figure S9). Of course, it is well established that HS Fe(II) complexes are labile in aqueous solution, and less so in the LS state.[31] Since **2** has a larger HS fraction than **1**, ligand dissociation might be more likely for the tetraphenylborate salt. The NMR spectra for **2** are very similar when collected on freshly prepared solutions without delay and after 1 day (Supporting Information, Figure S9); however, an observed decrease in $\chi_M T$ value (by 0.1 $emu \cdot K \cdot mol^{-1}$) over that time period implies that LS species are being produced, although we do not currently know the details of this rearrangement process. Thus, we readily acknowledge that ligand dissociation certainly takes place in **2** (and perhaps **1**) over a long time period (days), but this process is not likely to affect anion recognition studies carried out on fresh solutions.

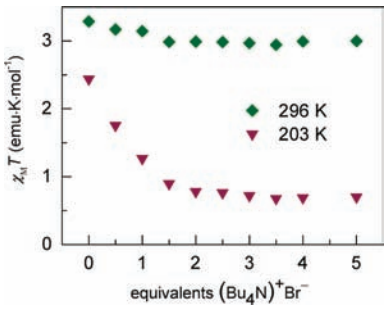

Figure 5. Changes in magnetic susceptibility upon addition of $^nBu_4NBr$ to CD_2Cl_2 solutions of **2** at 296 and 203 K, respectively.

The room temperature electronic absorption spectra for $[(H_2bip)_2Fe(pic)]^{2+}$ also vary as a function of anion (Figure 4b). When the charge balancing anion is changed from BPh_4^- to Br^-, the main peak shifts to the red (412 to 459 nm) and increases in intensity. This color change is consistent with an increase in LS population for the bromide salt, since charge transfer bands tend to be stronger and bluer for LS Fe(II) complexes. We also note that an increase in hydrogen bonding interactions for the bromide salt would increase the basicity of the H_2bip ligand, which could alter the energies of the charge-transfer bands without affecting the spin state.

Complex-Anion Interactions in Solution. Since we are primarily interested in testing the mixed ligand strategy for increasing operating temperatures rather than maximizing host−guest binding, we have focused anion binding studies on bromide, since our previous reports show that H_2bip complexes of Fe(II) are moderately selective for Br^- over Cl^-, I^-, NO_3^-, and ClO_4^-.[9,10] At room temperature, CD_2Cl_2 solutions of the tetraphenylborate salt **2** show a very modest decrease in $\chi_M T$ value (−0.34 $emu \cdot K \cdot mol^{-1}$) after the addition of 3.5 equiv of $^nBu_4NBr$ (Figure 5). The Fe(II) spin-state change is much more pronounced at 203 K, where $\chi_M T$ decreases from 2.44 to 0.68 $emu \cdot K \cdot mol^{-1}$ upon addition of 3.5 equiv of bromide. This change in measured susceptibilities indicates that the anion binding event causes spin-state switching from HS to LS at reduced temperatures. After adding more than 3.5 equiv of bromide, the $\chi_M T$ values show slight *increases* of 0.06 and 0.02 $emu \cdot K \cdot mol^{-1}$ at 296 and 203 K, respectively, which suggest the formation of some ligand dissociation products. The reformation of $[(H_2bip)_2FeBr_2]$ has been observed when another heteroleptic complex, $[(H_2bip)_2Fe(pipi)](BPh_4)_2$ (pipi = 2-pyridinalisopropylimine), has been titrated with excess $^nBu_4NBr$ under identical conditions.[10] Definitive confirmation that this occurs with the pic analogue is thwarted by overlapping signals in the ^1H NMR spectra.

As an alternative probe of complex-anion interactions, anion titrations for **2** can be monitored by electronic absorption spectroscopy. Consistent with the UV−visible spectra of the BPh_4^- and Br^- salts described above,

(29) (a) Berry, J. F.; Cotton, F. A.; Lu, T.; Murillo, C. A. *Inorg. Chem.* **2003**, *42*, 4425–4430. (b) Ozarowski, A.; Zvyagin, S. A.; Reiff, W. M.; Telser, J.; Brunel, L.-C.; Krzystek, J. *J. Am. Chem. Soc.* **2004**, *126*, 6574–6575.

(30) (a) Bryliakov, K. P.; Duban, E. A.; Talsi, E. P. *Eur. J. Inorg. Chem.* **2005**, 72–76. (b) England, J.; Britovsek, G. J. P.; Rabadia, N.; White, A. J. P. *Inorg. Chem.* **2007**, *46*, 3752–3767.

(31) Taube, H. *Chem. Rev.* **1952**, *50*, 69–126.

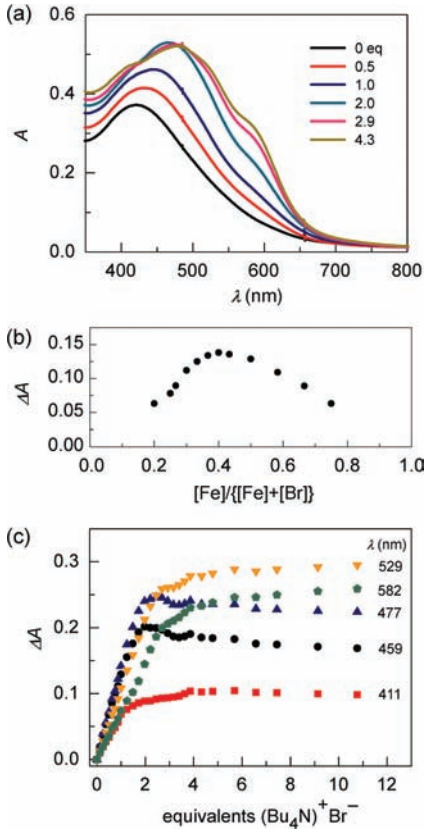

Figure 6. Electronic absorption changes for **2** (CH_2Cl_2, 296 K) upon titration of $^nBu_4NBr$: (a) visible spectral changes; (b) Job plot at 459 nm; (c) binding isotherms at selected wavelengths.

titrations of **2** with bromide significantly shift both absorption maxima and peak intensities after the addition of 2 equiv of $^nBu_4NBr$ (Figure 6a). However, the spectra do not evolve as simply as **2**→**1**, but instead continue to change when more than 2 equiv of bromide are added. Among other changes, a shoulder at ~582 nm increases in intensity. This feature is not found in pure **1** nor **2** (Figure 4b), but is observed when dichloromethane solutions of **1** are mixed with excess $^nBu_4NBr$ (Supporting Information, Figure S10a). Clearly, at least one new Fe-containing species is formed in the presence of excess bromide.

Considering the nature of solution speciation, the Job plot for mixtures of **2** and $^nBu_4NBr$ collected at 459 nm shows a species with 2:3 Fe:Br stoichiometry is the most stable (Figure 6b). This does not correspond to an obvious assembly of complexes and bromide, given that there are at least two strong (H_2bip) binding sites on each Fe complex; attempts to isolate this species have not been successful thus far. We note the relative flatness of the peak in the Job plot usually indicates weak binding,[32] but may also be consistent with the presence of multiple species with similar stabilities. Binding isotherms for **2** shown at selected wavelengths (Figure 6c) are also complex. The sharp increases in ΔA values for the addition of the first 2 equiv of Br^- indicate a strong binding event, which, by analogy to the bromide binding isotherms for $[Fe(H_2bip)_3]^{2+}$,[9] suggests bromide is first bound by the H_2bip ligand. Decreases in absorbance have been correlated to the formation of $[(H_2bip)_2FeBr_2]$, which is much less strongly absorbing than $[(H_2bip)_2Fe(NN)]^{2+}$ (NN = ancillary ligand) complexes in the visible electronic spectrum.[10] However, in the case of **2** not all the signals decrease in intensity (Figure 6c). As with the NMR experiments, we cannot rule out ligand dissociation, but neither can we confirm it. Bromide binding isotherms with **1** as the "host" show similar changes in absorbance (Supporting Information, Figure S10b). This complex behavior precludes facile determination of bromide binding constants.

Our work with the pic-containing heteroleptic complex has uncovered intriguing links between anion titrations and magnetic properties. By ligand field considerations, the anion-responsive working temperature for $[(H_2bip)_2Fe(pic)]^{2+}$ should be greater than that found for $[Fe(H_2bip)_3]^{2+}$. Instead, the temperature is significantly lower (H_2bip, −40 °C; pic, −70 °C). We recognize that the simple ligand field determinations used here only correspond to a d orbital gap, not absolute orbital energies. Perhaps the structural dissimilarity between pic (comprising amine and pyridine groups) and the other ancillary ligands used in previous studies[9,10] (diimines) diminishes the significance of ligand field considerations, since the functional groups interact with the Fe(II) center in different ways. However, Br^- titration of the homoleptic complex $[Fe(pic)_3]^{2+}$ shows a moderate *decrease* in $\chi_M T$ (i.e., lowering of spin state) under identical conditions as that employed for **2**,[33] suggesting that any hydrogen bonding interactions mediated by pic, at the minimum, do not destabilize the LS state.[34]

An alternative answer takes into account the following considerations. First, the Job plot for **2** combined with bromide suggests some kind of dimerization or other aggregation of Fe-containing complexes in solution. In addition, complex **1** displays concentration-dependent UV−visible spectra, in which the charge transfer band shifts from 463 to 451 nm when diluting from 0.61 to 0.15 mM (Supporting Information, Figure S11), suggesting the possibility of an aggregation effect in solution.[35] Second, both the H_2bip and pic ligands have the ability to interact with anions via hydrogen bonding, which is clearly evident in the solid state. Third, when the bromide salts of the $[(H_2bip)_2Fe(pic)]^{2+}$ complex are arranged differently in the solid state, they show drastically different temperature-dependent spin behaviors, even though local interactions are rather similar; importantly, solvate molecules in the structures appear to *dilute* any inductive effects imparted by bromide anions on the Fe complex spin state.

On the basis of these observations, we propose that additional supramolecular interactions in dichloromethane solution beyond the expected H_2bip-Br^- chelation are driven by the hydrogen bonding ability of the pic ligand. The pic ligand can share a bromide with an H_2bip ligand on a neighboring complex: it is observed in the solid state, it is not unreasonable in solution. Such sharing is not observed in the homoleptic complex $[Fe(H_2bip)_3]^{2+}$ (we have not found any structural evidence that two H_2bip ligands can share a bromide anion), otherwise

(32) MacCarthy, P. *Anal. Chem.* **1978**, *50*, 2165–2165.

(33) We observe a decrease in magnetic susceptibility after the addition of 3 equiv of bromide to $[Fe(pic)_3]Br_2 \cdot C_2H_5OH$ in CD_3CN at room temperature; however, the low solubility prevents us from determining an exact value. Importantly, we do not see an increase in magnetic susceptibility.

(34) Chum, H. L.; Vanin, J. A.; Holanda, M. I. D. *Inorg. Chem.* **1982**, *21*, 1146–1152.

(35) Kiriy, N.; Bocharova, V.; Kiriy, A.; Stamm, M.; Krebs, F. C.; Adler, H.-J. *Chem. Mater.* **2004**, *16*, 4765–4771.

similar aggregation might have been observed earlier. When bromide is shared between complexes, it cannot influence the H_2bip ligand field as strongly as if it is bound by one complex—its effect is diluted—and therefore the anion "sensing" is shifted to lower temperatures.

Conclusion and Outlook

We have prepared salts of new heteroleptic $[(H_2bip)_{2-n}Fe(pic)_{1+n}]^{2+}$ complexes, and find that they display a wide range of spin-state behaviors in the solid state as well as anion-dependent spin-state switching properties in solution. The solid state spin behaviors are heavily influenced by anion and solvate species, and are correlated with inner molecular structures (ligand field considerations), intermolecular interactions, and packing effects. The anion-binding-induced spin-state switching phenomenon can be found for $[(H_2bip)_2Fe(pic)]^{2+}$ in CD_2Cl_2 solution at 203 K, a significantly lower temperature than what would be expected based on ligand field considerations alone.

It is rare to have compounds in hand where solution and solid state investigations can be combined to improve understanding of spin-state behavior. The results presented here open a window onto the subtle intermolecular interactions that contribute to spin-state switching properties. Further advances require the synthesis of species that can be definitively shown to remain intact in solution. Notwithstanding, the $[(H_2bip)_2Fe(pic)]^{2+}$ complex is appealing in that ligand field and anion—cation interactions are balanced in a regime where supramolecular effects can be probed. The preparation and study of robust analogues of $[(H_2bip)_2Fe(pic)]^{2+}$ are in progress.

Acknowledgment. This research was supported by Colorado State University and the ACS Petroleum Research Fund (44691-G3). We thank Prof. S. H. Strauss for helpful comments.

Supporting Information Available: X-ray structural data (cif); details of the asymmetric unit in the crystal structure (pdf). This material is available free of charge via the Internet at http://pubs.acs.org.